

## Chapter 2

# Surface Recombination Theory

*If it is true that every theory must be based upon observed facts, it is equally true that facts cannot be observed without the guidance of some theory. Without such guidance, our facts would be desultory and fruitless; we could not retain them: for the most part we could not even perceive them.*

— Isidore Auguste Marie François Xavier Comte  
THE POSITIVE PHILOSOPHY

In order to provide a theoretical background for subsequent experimental chapters, we begin in this chapter with a review of the physical theory relevant to semiconductor surface recombination. We start with a discussion of the mechanisms of surface recombination and passivation, and review the conceptual picture of the semiconductor–dielectric interface. We proceed to the definition of the relevant energies and potentials, before describing the calculation of the surface carrier concentrations in the presence of charge-induced band-bending. We then introduce the equations describing recombination at the semiconductor surface, and discuss some simplifying cases. Finally we describe how the experimental parameters commonly used to characterise surface recombination relate to the physical properties of the interface.

Familiarity with basic semiconductor physics is assumed, as necessarily only brief and partial coverage of such topics is provided here. Many excellent texts on this subject exist (see for example [1–4]). For a more extensive discussion of surface recombination theory (albeit covering somewhat different ground) see the work of Aberle [5].

### 2.1 The Semiconductor Surface

At the surface of a semiconductor, the atomic lattice is abruptly interrupted. Surface atoms lack neighbours to bind to, and are left with unsatisfied “dangling” bonds (unpaired outer-shell electrons). These dangling bonds introduce electronic energy

levels inside the normally forbidden semiconductor bandgap, referred to as surface or interface states.<sup>1</sup> Such states greatly enhance electron–hole recombination at the surface by acting as stepping stones for charge carrier transitions between the conduction and valence bands.

The reduction of surface recombination is referred to as surface passivation. Since each recombination event at the surface requires, in addition to an interface state, precisely one electron and one hole, the two fundamental approaches to passivation are

1. to reduce the number of interface states, or
2. to reduce the concentration of one or other carrier at the surface.

The first of these approaches, usually referred to as “chemical” passivation, is generally accomplished by the formation of a thin layer of a wide-bandgap material on the semiconductor surface, such that most previously dangling bonds are chemically bound to atoms within this layer. The material in question may be a dielectric (e.g.  $\text{SiO}_2$ ,  $\text{SiN}_x$ ,  $\text{Al}_2\text{O}_3$ ), or it may be another semiconductor, or even the same semiconductor in a different structural form (e.g. amorphous Si on a crystalline Si surface). Additional dangling bonds may often be passivated by hydrogen atoms, either sourced from within the passivating layer itself or externally via a hydrogen anneal. By this means, interface state density may be reduced to extremely low levels,<sup>2</sup> though not entirely eliminated.

The second approach, of reducing the concentration of one type of carrier at the surface, may be accomplished in several different ways. Firstly, the surface concentration of one carrier may be reduced by the application of a field to the surface that repels that type of carrier. This field may be the result of an externally applied bias in a MIS structure, or of inbuilt stable charges within a passivating dielectric layer or stack. Passivation effected in this way may be referred to as “field-effect” or “charge-assisted” passivation.

Alternatively, such a reduction of the surface carrier concentration may be achieved by the formation of a heavily doped region at the semiconductor surface, which suppresses the concentration of one carrier type due to the change in chemical potential. Such a doped region may be formed by the introduction of dopant atoms (most commonly B, P, and Al in silicon) via thermal diffusion, ion implantation, or alloying. The most well-known example of this effect is the so-called “back-surface field”,<sup>3</sup> or high–low junction, commonly formed by alloying of Al at the rear of conventional  $p$ -type silicon solar cells during the high-temperature contact firing step.

Finally, the concentration of minority carriers at the surface may be suppressed by reducing the minority carrier mobility in the near-surface region of the semiconductor,

---

<sup>1</sup>In the case of a bare surface the interface in question is between the semiconductor and the surrounding ambient.

<sup>2</sup>Concentrations as low as a few  $10^9 \text{ eV}^{-1} \text{ cm}^{-2}$  have been reported for Si– $\text{SiO}_2$  [6], compared to surface bond densities on the order of  $10^{14} \text{ cm}^{-2}$ .

<sup>3</sup>Although widespread in use, this term is a significant historical misnomer, as clearly explained by [7]. In reality the passivation effect involved has little to do with any field.

such that the surface concentration becomes transport-limited. This mechanism is significant, for example, in heavily doped diffused regions, where it operates in conjunction with the doping mechanism described above to reduce the minority carrier concentration at the surface.

The two basic approaches to surface passivation described above are not mutually exclusive, and indeed are typically employed in combination to minimise surface recombination in actual devices. For example, conventional *p*-type silicon solar cells feature a phosphorus-diffused *n*+ region on their front surface, which apart from performing a charge-separation role, also acts to suppress the surface hole concentration. Outside of the contacted regions, this surface is also passivated by a dielectric layer (PECVD  $\text{SiN}_x$ ), which both reduces the interface state concentration and contains positive fixed charges which induce further charge-assisted passivation. It is the recombination at such semiconductor–dielectric interfaces that we shall be concerned with here.

The use of dielectric surface passivation was first reported by Atalla et al. [8] in 1959, who discovered that the formation of a thermally grown  $\text{SiO}_2$  layer greatly reduced the concentration of electronic states at the silicon surface. An enormous amount of work on understanding the electrical properties of silicon–dielectric interfaces, especially that of  $\text{SiO}_2$ , was performed during the following decades, primarily motivated by applications in microelectronics. This work resulted in the emergence of a well-established conceptual picture of such interfaces, along with a standard nomenclature describing them.

Important general results of this work are that:

- Defects at the disordered semiconductor–dielectric interface, unlike those in the well-ordered crystalline bulk, give rise to an energetic continuum of states distributed throughout the bandgap, due to the influence of small variations in the chemical environment of each defect, and the existence of multiple species of states.
- Such states may be donor- or acceptor-like (the former are positively charged when empty, and neutral when occupied by an electron, while the latter are neutral when empty and negatively charged when occupied).
- For typical concentrations, these states are non-interacting (because their spatial separation makes electron transitions extremely unlikely).<sup>4</sup>
- Additional permanently charged states, known as “fixed charges”, are typically present in the dielectric near the interface. These do not exchange charge with the semiconductor and are not recombination-active. However, they do contribute to charge-assisted surface passivation.

---

<sup>4</sup>A partial exception to this are so-called “amphoteric” defects, where a single physical defect contributes two energy levels within the semiconductor bandgap. A well-known example is the so-called  $\text{P}_b$  defect at the Si– $\text{SiO}_2$  interface [9].

## 2.2 Definition of Energies and Potentials

Preliminary to a discussion of the equations describing recombination, it is necessary to define the terms that we will be using for the various energies and potentials involved. Figure 2.1 shows the band diagram of a  $p$ -type silicon surface under non-equilibrium conditions, with the surface in accumulation.  $E_c$  and  $E_v$  are the energies of the conduction and valence band edges respectively, with the bandgap energy  $E_g = E_c - E_v$ .  $E_{Fn}$  and  $E_{Fp}$  are the energies of the quasi-Fermi-levels for electrons and holes, defined such that

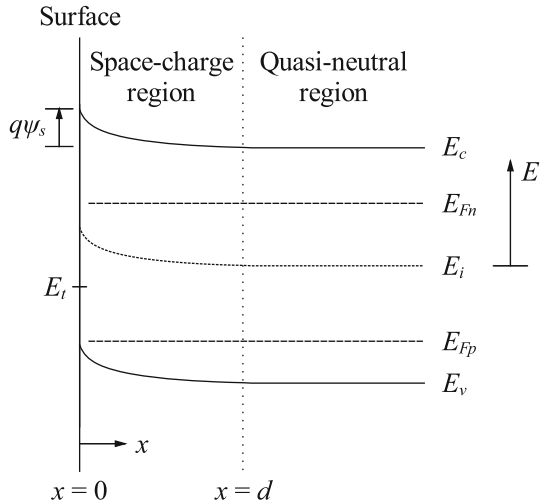
$$n = N_c F_{1/2} \left( \frac{E_{Fn} - E_c}{kT} \right), \quad (2.1)$$

$$p = N_v F_{1/2} \left( -\frac{E_{Fp} - E_v}{kT} \right), \quad (2.2)$$

where  $n$  and  $p$  are the free electron and hole concentrations,  $N_c$  and  $N_v$  are the effective densities of states in the conduction and valence bands,  $k$  is the Boltzmann constant, and  $T$  is the temperature in Kelvin.  $F_j(\eta)$  is the Fermi–Dirac integral of the  $j$ th order, defined by

$$F_j(\eta) = \frac{1}{\Gamma(j+1)} \int_0^\infty \frac{\varepsilon^j}{1 + \exp(\varepsilon - \eta)} d\varepsilon, \quad (2.3)$$

**Fig. 2.1** Band diagram of the ( $p$ -type) silicon surface under non-equilibrium conditions, and with non-zero surface band-bending (*accumulation*), showing definitions of relevant energies and potentials



which must generally be solved numerically. However, excellent analytical approximations for (2.3) are available [10, 11] and readily implemented in numerical software.

The intrinsic Fermi energy  $E_i$  is defined as the energy for which  $n = p = n_i$  when  $E_{Fn} = E_{Fp} = E_i$ , where  $n_i$  is the intrinsic carrier concentration. For carrier concentrations much less than the relevant density of states, Eqs. (2.1) and (2.2) may be approximated by their nondegenerate (Boltzmann) forms:

$$n = N_c \exp\left(\frac{E_{Fn} - E_c}{kT}\right) = n_i \exp\left(\frac{E_{Fn} - E_i}{kT}\right), \quad \text{for } n \ll N_c, \quad (2.4)$$

$$p = N_v \exp\left(-\frac{E_{Fp} - E_v}{kT}\right) = n_i \exp\left(-\frac{E_{Fp} - E_i}{kT}\right), \quad \text{for } p \ll N_v, \quad (2.5)$$

In this work we make use of the values of  $E_g$  and  $N_c$  recommended by Green [12] for crystalline silicon. The value of  $N_v$ , which is known with less confidence [12], is calculated to be consistent with these values and with the value for  $n_i$  of Misiakos and Tsamakis [13].

## 2.3 Surface Charge and Band-Bending

The presence of external net charge in an overlying dielectric layer or gate contact, or trapped in interface states, induces a compensating net charge in the semiconductor, distributed over a spatially extended region near the surface. This “space-charge region” may take the form of either an accumulation layer, inversion layer, or depletion region, depending on whether the dominant contribution to the charge comes from majority free carriers, minority free carriers, or uncompensated ionised dopant atoms respectively. It appears in the band diagram of Fig. 2.1 as a bending of the semiconductor energy bands near the surface. The extent of this band-bending is described by the surface potential  $\psi_s$ , which is positive for downward band-bending towards the surface. Further from the surface, approximate charge neutrality prevails, and the semiconductor is said to be in a quasi-neutral state. The boundary between the quasi-neutral and space-charge regions is located at a distance  $d$  from the surface.

Charge neutrality requires that the total net charge in the space-charge region,  $Q_s$ , precisely balance the total external charge  $Q_{tot}$ , such that  $Q_s + Q_{tot} = 0$ . Most commonly,  $Q_{tot}$  may include contributions from insulator fixed charge  $Q_f$ , interface trapped charge  $Q_{it}$ , and charge in the gate contact  $Q_g$ . The latter is absent in many photovoltaic test structures and devices, which lack a gate contact, while  $Q_{it}$  is typically negligible at well-passivated surfaces, so that  $Q_{tot}$  is dominated by  $Q_f$ .

Typically, we know  $Q_{tot}$  and hence  $Q_s$  (usually from C–V measurements), and wish to determine the surface carrier concentrations  $p_s$  and  $n_s$ . In order to determine the extent of band-bending, and hence the surface carrier concentrations, we must start from the carrier concentrations at the edge of the quasi-neutral region. In non-equilibrium, we have

$$n_d = n_{0d} + \Delta n_d, \quad (2.6)$$

$$p_d = p_{0d} + \Delta n_d, \quad (2.7)$$

where  $n_0$  and  $p_0$  are the equilibrium concentrations of electrons and holes respectively, and  $\Delta n$  is the excess carrier concentration. The subscript  $d$  indicates that these parameters are referenced to the edge of the quasi-neutral region.

$n_0$  and  $p_0$  may be calculated from (2.1) and (2.2) together with the equilibrium condition ( $E_{Fn} = E_{Fp}$ ) and the requirement of charge neutrality:

$$n_0 + N_A = p_0 + N_D, \quad (2.8)$$

where  $N_D$  and  $N_A$  are the active donor and acceptor concentrations respectively. For a uniformly doped sample with surface recombination that is not very large,  $\Delta n_d$  is simply equal to its average bulk value,  $\Delta n$ , which is typically known directly from experiment. In other cases, such as when a diffused surface dopant profile is present,  $\Delta n_d$  must first be calculated separately. In the general case, this requires a numerical solution of the coupled semiconductor equations over the surface dopant profile, taking into account local variation of the carrier mobility, recombination, and bandgap narrowing, as described by [14–16]. Given  $n_d$  and  $p_d$ , the corresponding values of  $E_{Fn}$  and  $E_{Fp}$  may then be calculated from (2.1) and (2.2).

Having determined  $E_{Fn}$  and  $E_{Fp}$  in the quasi-neutral region, we need an expression relating the semiconductor charge  $Q_s$  to the surface potential  $\psi_s$ . This requires a solution of Poisson's equation in one dimension. For Fermi–Dirac statistics we obtain [17]

$$\begin{aligned} Q_s = (2kT\epsilon_s)^{1/2} & \left\{ N_c \left[ F_{3/2} \left( \frac{E_{Fn} - E_c + q\psi_s}{kT} \right) - F_{3/2} \left( \frac{E_{Fn} - E_c}{kT} \right) \right] \right. \\ & + N_v \left[ F_{3/2} \left( \frac{E_v - E_{Fp} - q\psi_s}{kT} \right) - F_{3/2} \left( \frac{E_v - E_{Fp}}{kT} \right) \right] \\ & \left. + (N_A - N_D) \left( \frac{q}{kT} \psi_s \right) \right\}^{1/2}. \end{aligned} \quad (2.9)$$

Under nondegenerate conditions this may be approximated by

$$\begin{aligned} Q_s = (2kT\epsilon_s)^{1/2} & \left\{ N_c \left[ \exp \left( \frac{E_{Fn} - E_c + q\psi_s}{kT} \right) - \exp \left( \frac{E_{Fn} - E_c}{kT} \right) \right] \right. \\ & + N_v \left[ \exp \left( \frac{E_v - E_{Fp} - q\psi_s}{kT} \right) - \exp \left( \frac{E_v - E_{Fp}}{kT} \right) \right] \\ & \left. + (N_A - N_D) \left( \frac{q}{kT} \psi_s \right) \right\}^{1/2}. \end{aligned} \quad (2.10)$$

Given  $Q_s$ , Eq. (2.9) or (2.10) must be solved iteratively to determine  $\psi_s$ , in the manner described by [18]. The surface carrier concentrations may then be calculated using either (2.1) and (2.2), or (2.4) and (2.5), as appropriate.

Finally, we note that Eq. (2.10) is equivalent to

$$Q_s = (2kT\epsilon_s)^{1/2} \{n_s - n_d + p_s - p_d + (N_A - N_D) [(kT/q)^{-1} \psi_s]\}^{1/2}. \quad (2.11)$$

For large  $Q_s$ , the  $n_s$  and  $p_s$  terms in (2.11) dominate [19], so that at a strongly  $p$ -type surface we have

$$p_s = Q_s^2 (2kT\epsilon_s)^{-1}, \quad (2.12)$$

i.e. the majority surface carrier concentration is simply proportional to  $Q_s^2$ . This useful result will be employed later to provide a simple analytical expression for surface recombination at charge-passivated surfaces.

## 2.4 Recombination Through Defect States

The net rate of excess carrier recombination arising from non-interacting single-level states in the semiconductor bandgap is described by the well-known Shockley–Read–Hall (SRH) statistics [20, 21]. For a single state located at energy  $E_t$ , the recombination rate  $U_{SRH}$  is given by

$$U_{SRH} = \frac{pn - n_i^2}{c_p^{-1}(n + n_1) + c_n^{-1}(p + p_1)}, \quad (2.13)$$

where  $c_n$  and  $c_p$  are the capture coefficients for electrons and holes, and  $n_1$  and  $p_1$  are the equilibrium electron and hole concentrations for the case where  $E_{Fn} = E_{Fp} = E_t$ , given by

$$n_1 = N_c F_{1/2}((E_t - E_c)/kT), \quad (2.14)$$

$$p_1 = N_v F_{1/2}(-(E_t - E_v)/kT). \quad (2.15)$$

These last terms account for re-emission of trapped carriers, which occurs in competition with recombination, and have the effect of reducing the recombinative effectiveness of states located close to the band edges. For states not very near the band edges,  $n_1$  and  $p_1$  may be approximated by their nondegenerate forms, and  $F_{1/2}$  in (2.14) and (2.15) may be replaced by an exponential term.

The numerator in Eq. (2.13) ( $pn - n_i^2$ ) describes the displacement of the carrier concentrations from thermal equilibrium, which is the driving force for net recombination or generation (the latter occurring for  $pn < n_i^2$ ).

The capture coefficients describe the capture probability per unit time for a free electron or hole in the vicinity of the state, and may be thought of as relating to the

effective cross-sectional area of the potential well formed by the defect, referred to as the capture cross-section, and designated by  $\sigma_n$  and  $\sigma_p$  for electrons and holes respectively. We may write

$$c_n = \sigma_n v_{th}, \quad (2.16)$$

where  $v_{th}$  is the thermal velocity of the carrier in question (an analogous equation may be written relating  $c_p$  to  $\sigma_p$ ). As the capture coefficient is both the experimentally determined value and the value relevant to recombination, and the value of  $v_{th}$  is somewhat contentious, the concept of capture cross-sections is of limited utility, beyond providing a conceptual aid, and the choice of  $v_{th}$  is somewhat arbitrary. However, this mode of representation is widely used in the literature. Since different authors make various assumptions concerning the value of  $v_{th}$ , capture cross-section values in the literature should be compared with care.

## 2.5 Surface Recombination

At the semiconductor surface we can write a similar equation to (2.13) for recombination through a single interface state:

$$U_s = \frac{p_s n_s - n_i^2}{c_p^{-1}(n_s + n_1) + c_n^{-1}(p_s + p_1)}, \quad (2.17)$$

where the subscript  $s$  denotes that these properties relate to the surface.

The total recombination rate is found by summing the contributions of the individual states. At the surface this involves an integration over energy, due to the energetic continuum of interface states. Integrating (2.17) over energy  $E$  for all interface states within the semiconductor bandgap yields

$$U_s = \int_{E_v}^{E_c} D_{it} \frac{p_s n_s - n_i^2}{c_p^{-1}(n_s + n_1) + c_n^{-1}(p_s + p_1)} dE, \quad (2.18)$$

where  $D_{it}$  is the areal density of interface states as a function of energy. Note that besides  $D_{it}$ ,  $c_p$ ,  $c_n$ ,  $n_1$ , and  $p_1$  are also functions of energy, though we have omitted this dependence from (2.18) for the sake of brevity.

In Eq. (2.18), we have assumed that all surface states at a given energy have the same  $c_n$  and  $c_p$ . In general however, this is unlikely to be the case. Instead, multiple types of surface state (arising from distinct chemical sites) with overlapping energy distributions and distinct capture properties are likely to be present. We must then calculate  $U_{s,total}$  as the sum of contributions due to each distribution:

$$U_{s,total} = \sum_{i=1}^n U_{s,i}. \quad (2.19)$$



### Limiting Cases

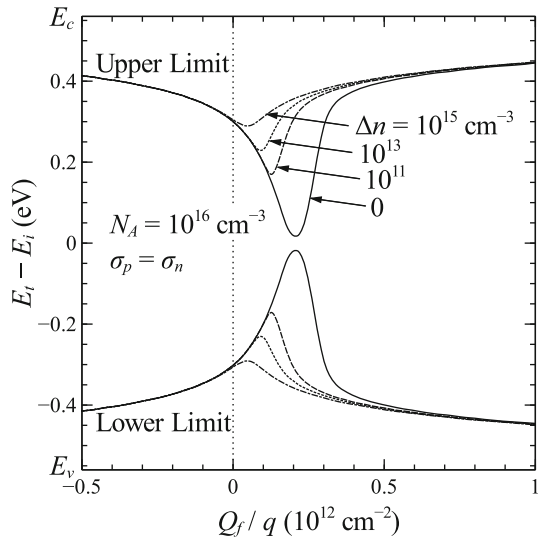
It is worthwhile to consider some limiting cases under which Eq. (2.18) may be simplified. Such cases occur frequently in practice and aid considerably in exposing the functional dependencies involved.

The first point to note is that  $p_1$  and  $n_1$  may frequently be neglected for interface states not very close to the band edge, since they are insignificant compared to either  $p_s$  or  $n_s$ . This will be the case when either (1) the excess carrier concentration  $\Delta n$  is large, or (2) the surface is in strong accumulation or inversion, such that  $p_s$  or  $n_s$  is large, regardless of  $\Delta n$ .

Illustrating this case, Fig. 2.2 shows the bandgap energy range over which interface state recombination efficiency is greater than 90% of its midgap value, as a function of surface charge and of excess carrier concentration. A bulk acceptor concentration  $N_A = 10^{16} \text{ cm}^{-3}$  and equal capture cross-sections for electrons and holes are assumed (the effect of increasing dopant concentration is to stretch out the curves on the  $Q_f/q$  axis). When the surface is in depletion, the recombination efficiency of interface states not near midgap is strongly reduced due to competing re-emission of trapped carriers. However, this effect is substantially suppressed when the bulk excess carrier concentration is significant, as under illumination. In accumulation or strong inversion, emission processes are important only for states located near the band edges, regardless of bulk injection.

For the case shown in Fig. 2.2, interface states in the middle 0.7 eV or more of the bandgap contribute equally to recombination for  $Q_f/q > 2.5 \times 10^{11} \text{ cm}^{-2}$  or  $Q_f/q < -1 \times 10^{11} \text{ cm}^{-2}$ , even at a low injection level of  $\Delta n = 10^{11} \text{ cm}^{-3}$ . These charge magnitudes are significantly smaller than those typically encountered at silicon–dielectric interfaces, even in the case of  $\text{SiO}_2$ , which is usually considered

**Fig. 2.2** Bandgap energy range over which interface state recombination is greater than 90% of the midgap value, as a function of insulator fixed charge  $Q_f$  and with bulk excess carrier concentration  $\Delta n$  as a parameter. We assume  $N_A = 10^{16} \text{ cm}^{-3}$  and  $\sigma_p = \sigma_n$



to possess a rather low charge. Additionally, interface states located closer to the band edges are generally found to possess rather low capture cross-sections [4], so that they are unimportant for recombination regardless of band-bending. Consequently, the neglect of  $p_1$  and  $n_1$  is frequently justified in determining surface recombination.

Secondly, in many cases of interest the concentration of one or other carrier will be dominant at the surface, such that recombination is limited by the rate of minority carrier capture. Taking the case of a strongly  $p$ -type surface ( $c_p p_s \gg c_n n_s$ ), and neglecting  $p_1$  and  $n_1$  for the reasons described above, Eq. (2.18) reduces to

$$U_s = \frac{p_s n_s - n_i^2}{p_s} \int_{E_v}^{E_c} D_{it} c_n dE \quad (2.20)$$

The integral in (2.20) now contains all the terms relating to the interface state properties, and no others. It therefore encapsulates the *chemical* passivation of the interface. Noting that the integral has units of velocity, we may define a fundamental surface recombination velocity of electrons  $S_{n0}$ , given by

$$S_{n0} = \int_{E_v}^{E_c} D_{it} c_n dE. \quad (2.21)$$

The conditions relating to Eq. (2.20) will hold for all  $p$ -type surfaces and most undiffused  $n$ -type surfaces passivated by a negatively charged dielectric such as  $\text{Al}_2\text{O}_3$ . An analogous expression for  $U_s$  in terms of  $S_{p0}$  may be derived for strongly  $n$ -type surfaces.

### $S_{\text{eff}}$ and $J_0$ s

Because the surface carrier concentrations  $p_s$  and  $n_s$  are generally not known, it is common to describe surface recombination in terms of an effective surface recombination velocity  $S_{\text{eff}}$ , defined with respect to the excess (non-equilibrium) carrier concentration  $\Delta n_d$  at the edge of the quasi-neutral region of the semiconductor,

$$S_{\text{eff}} \equiv \frac{U_s}{\Delta n_d}. \quad (2.22)$$

From (2.20) to (2.22),  $S_{\text{eff}}$  is related to  $S_{n0}$  via

$$S_{\text{eff}} = S_{n0} \frac{p_s n_s - n_i^2}{p_s \Delta n_d} \approx S_{n0} \frac{n_s}{\Delta n_d}, \quad (2.23)$$

where the latter expression applies when the surface carrier concentration is far from thermal equilibrium ( $p_s n_s \gg n_i^2$ ). For surfaces not in inversion, i.e. where the surface minority carriers are the same as those in the near-surface quasi-neutral region, we can make the further substitution  $\Delta n_d \approx n_d$ . Note that it is not necessary to include bandgap narrowing in the calculation of  $n_s$  and  $p_s$  in (2.23), so long as this effect is approximately constant over the surface space-charge profile induced by  $Q_f$ .

Making the substitution  $p_s n_s \approx (n_s + \Delta n_d) \Delta n_d$ , (2.23) can be rewritten as

$$S_{eff} = S_{n0} \frac{(n_s + \Delta n_d)}{p_s}, \quad (2.24)$$

where we have assumed that the surface dopant concentration  $n_s$  is equal to that at the edge of the quasi-neutral region. Using the approximate expression for  $p_s$  provided by Eq. (2.12) when  $Q_f$  is large and the carrier concentrations are nondegenerate, this becomes

$$S_{eff} = S_{n0} \frac{2kT\epsilon_s}{Q_s^2} (n_s + \Delta n_d). \quad (2.25)$$

Equation (2.25) shows that  $S_{eff}$  in this case is dependent on both the dopant concentration and the injection level. This limits the usefulness of  $S_{eff}$  as a means of characterising surface recombination, as discussed by [19].

As an alternative to  $S_{eff}$ , we may instead describe surface recombination in terms of the surface saturation current density  $J_{0s}$ , defined by [19]

$$J_{0s} = qU_s \left( \frac{p_s n_s - n_i^2}{n_i^2} \right)^{-1}. \quad (2.26)$$

Combining (2.20), (2.21), and (2.26), we find, for a strongly  $p$ -type surface,

$$J_{0s} = qS_{n0} p_s^{-1} n_i^2. \quad (2.27)$$

Again using the high-charge, nondegenerate approximation for  $p_s$  given by (2.12), we obtain

$$J_{0s} = qS_{n0} \frac{2kT\epsilon_s}{Q_s^2} n_i^2. \quad (2.28)$$

$J_{0s}$  thus has the merit of being independent of the dopant concentration and injection level when the conditions relating to (2.28) hold, as they do frequently in practice for undiffused surfaces passivated by  $\text{Al}_2\text{O}_3$ .

## 2.6 Relationship to Experimental Parameters

Generally, one does not measure surface recombination directly, but rather the effective excess minority carrier lifetime  $\tau_{eff}$ , typically as a function of the average excess carrier concentration  $\Delta n$ .  $\tau_{eff}$  is defined by

$$\tau_{eff} \equiv \frac{\Delta n}{U_{total}}, \quad (2.29)$$

where  $U_{total}$  is the total volumetric recombination rate due to all mechanisms, both in the bulk and at the surface.  $\tau_{eff}$  can therefore be expressed as the parallel combination of the carrier lifetimes due these various recombination processes. We consider the case of a uniformly doped, undiffused sample. Then

$$\tau_{eff}^{-1} = \tau_{int}^{-1} + \tau_{SRH}^{-1} + \tau_s^{-1}, \quad (2.30)$$

where  $\tau_{int}$  is the intrinsic bulk lifetime due to radiative and Auger recombination [22],  $\tau_{SRH}$  is the extrinsic bulk lifetime due to SRH recombination through bulk defects, and  $\tau_s$  is the carrier lifetime due to surface recombination. For a symmetrically passivated, undiffused wafer,  $\tau_s$  is related to  $U_s$  by

$$\tau_s = \frac{W}{2} \frac{\Delta n}{U_s}. \quad (2.31)$$

where  $W$  is the wafer thickness, and  $U_s$  refers to the value at each surface. Equation (2.31) assumes that  $\Delta n$  is uniform throughout the width of the wafer, which may not hold if the generation profile is significantly nonuniform, or surface recombination is very large.

Combining Eqs. (2.22), (2.30), and (2.31), and using the fact that for undiffused surfaces  $\Delta n_d = \Delta n$ , we arrive at the following expression for  $S_{eff}$  in terms of  $\tau_{eff}$ :

$$S_{eff} = \frac{W}{2} \left( \frac{1}{\tau_{eff}} - \frac{1}{\tau_{int}} - \frac{1}{\tau_{SRH}} \right) \quad (2.32)$$

$S_{eff}$  determined from (2.32) is commonly used to characterise surface recombination at undiffused surfaces, and will be used extensively in the following chapters for this purpose. Since  $\tau_{SRH}$  is generally unknown, it is usually assumed that  $\tau_{SRH}^{-1} = 0$ , so that the calculated  $S_{eff}$  represents an upper limit.

For diffused surfaces, it is more common to describe the recombination rate in terms of a saturation current density  $J_0$ , analogous to the surface saturation current density  $J_{0s}$ , but defined with respect to the carrier concentrations at the edge of the diffused region, and including Auger and SRH recombination in the heavily doped diffusion in addition to SRH recombination at the surface. Assuming  $\Delta n \gg n_i$ , we may write [23]:

$$J_0 = qn_i^2(N_b + \Delta n)^{-1} \frac{W}{2} \left( \frac{1}{\tau_{eff}} - \frac{1}{\tau_{int}} - \frac{1}{\tau_{SRH}} \right), \quad (2.33)$$

where  $N_b$  is the bulk dopant concentration. The use of  $J_0$  rather than  $S_{eff}$  has the advantage that  $J_0$  is independent of  $\Delta n$  at such surfaces, so long as recombination at the surface itself remains limited by minority carrier capture [23]. Equation (2.33) may be used directly to calculate  $J_0$  from  $\tau_{eff}$  for a given  $\Delta n$ . However, this has the disadvantage that the extracted  $J_0$  includes  $\tau_{SRH}$ , since this is generally not known independently. Instead, assuming that  $J_0$  is independent of  $\Delta n$ , we may take the derivative of (2.33) with respect to  $\Delta n$ , leading to

$$J_0 = qn_i^2 \frac{W}{2} \frac{d}{d\Delta n} \left( \frac{1}{\tau_{eff}} - \frac{1}{\tau_{int}} - \frac{1}{\tau_{SRH}} \right). \quad (2.34)$$

$J_0$  may thus be determined from the linear slope of  $\tau_{eff}^{-1} - \tau_{int}^{-1}$  versus  $\Delta n$  [23]. This has the advantage that if the bulk is in high injection ( $\Delta n \gg N_b$ ),  $\tau_{SRH}$  is independent of  $\Delta n$ , so that the extracted  $J_0$  is unaffected by error due to extrinsic bulk recombination, even if such recombination is significant. Such conditions are readily obtained using high resistivity (lightly doped) substrates.

Although usually applied to characterise recombination at diffused surfaces,  $J_0$  determined from Eqs. (2.33) or (2.34) is also of use to characterise undiffused surfaces where surface recombination is dominated by minority carrier capture. For an undiffused wafer with uniform doping and injection,  $p_s n_s = (N_b + \Delta n) \Delta n$ , and therefore  $J_0 = J_{0s}$ . Thus, when the conditions relating to (2.20) apply,  $J_0$  derived from Eqs. (2.33) or (2.34) provides an injection-independent means of characterising surface recombination at undiffused surfaces.

Note that the measured quantity in all cases is, in fact,  $J_0/n_i^2$ , which is also the quantity relevant to recombination, and is essentially independent of temperature. Consequently, the choice of  $n_i$  used to extract  $J_0$  is arbitrary. We present results in terms of  $J_0$  rather than  $J_0/n_i^2$  only because this is the convention. It is however a trivial matter to apply a different value of  $n_i$  in order to make the  $J_0$  values comparable with those quoted by other authors using different values of  $n_i$ . In all cases in this work we use  $n_i$  given by [13] at 300 K ( $9.7 \times 10^9 \text{ cm}^{-3}$ ).

Finally, we note that by comparison of (2.32) and (2.33),  $S_{eff}$  is related to  $J_0$  by

$$S_{eff} = J_0 \frac{N_b + \Delta n}{qn_i^2}. \quad (2.35)$$

The methodology developed in this chapter will be employed in Chaps. 4–8 to characterise surface recombination experimentally, and to relate it to the physical parameters of the Si–Al<sub>2</sub>O<sub>3</sub> interface.

## References

1. Sze, S.M.: *Semiconductor Devices: Physics and Technology*, 3rd edn. Wiley, Hoboken (2002)
2. Pierret, R.F.: *Advanced semiconductor fundamentals*, 2nd edn. Pearson Education, Upper Saddle River (2003)
3. Würfel, P.W.: *Physics of Solar Cells: From Basic Principles to Advanced Concepts*, 2nd edn. Wiley-VCH, Weinheim (2009)
4. Nicollian, E.H., Brews, J.R.: *MOS (Metal Oxide Semiconductor) Physics and Technology*. Wiley, New York (1982)
5. Aberle, A.G.: *Crystalline Silicon Solar Cells: Advanced Surface Passivation and Analysis*. University of New South Wales, Sydney (1999)
6. Declerck, G., Overstraeten, R.V., Broux, G.: Measurement of low densities of surface states at the Si–SiO<sub>2</sub>-interface. *Solid-State Electron.* **16**, 1451–1460 (1973)

7. Cuevas, A., Yan, D.: Misconceptions and misnomers in solar cells. *IEEE J. Photovolt.* **3**, 916–923 (2013)
8. Atalla, M., Tannenbaum, E., Scheibner, E.: Stabilization of silicon surfaces by thermally grown oxides. *Bell Syst. Tech. J.* **38**, 749–783 (1959)
9. Poindexter, E.H.: MOS interface states: overview and physicochemical perspective. *Semicond. Sci. Technol.* **4**, 961–969 (1989)
10. Van Halen, P., Pulfrey, D.L.: Accurate, short series approximations to Fermi-Dirac integrals of order  $-1/2$ ,  $1/2$ ,  $1$ ,  $3/2$ ,  $2$ ,  $5/2$ ,  $3$ , and  $7/2$ . *J. Appl. Phys.* **57**, 5271–5274 (1985)
11. Van Halen, P., Pulfrey, D.L.: Erratum: Accurate, short series approximations to Fermi-Dirac integrals of order  $-1/2$ ,  $1/2$ ,  $1$ ,  $3/2$ ,  $2$ ,  $5/2$ ,  $3$ , and  $7/2$ . *J. Appl. Phys.* **59**, 2264–2265 (1986)
12. Green, M.A.: Intrinsic concentration, effective densities of states, and effective mass in silicon. *J. Appl. Phys.* **67**, 2944–2954 (1990)
13. Misiakos, K., Tsamakis, D.: Accurate measurements of the silicon intrinsic carrier density from 78 to 340 K. *J. Appl. Phys.* **74**, 3293–3297 (1993)
14. Van Overstraeten, R.J., DeMan, H.J., Mertens, R.P.: Transport equations in heavy doped silicon. *IEEE Trans. Electron Device.* **20**, 290–298 (1973)
15. del Alamo, J., Swanson, R.: The physics and modeling of heavily doped emitters. *IEEE Trans. Electron Device.* **31**, 1878–1888 (1984)
16. McIntosh, K., Altermatt, P.: A freeware 1D emitter model for silicon solar cells. In: Proceedings of the 35th IEEE Photovoltaic Specialists Conference, 2010, pp. 002 188–002 193
17. Seiwatz, R., Green, M.: Space charge calculations for semiconductors. *J. Appl. Phys.* **29**, 1034–1040 (1958)
18. Girisch, R.B.M., Mertens, R.P., De Keersmaecker, R.F.: Determination of Si-SiO<sub>2</sub> interface recombination parameters using a gate-controlled point-junction diode under illumination. *IEEE Trans. Electron Device.* **35**, 203–222 (1988)
19. McIntosh, K.R., Black, L.E.: On effective surface recombination parameters. *J. Appl. Phys.* **116**, 014503 (2014)
20. Shockley, W., Read, W.T.: Statistics of the recombinations of holes and electrons. *Phys. Rev.* **87**, 835–842 (1952)
21. Hall, R.N.: Electron-hole recombination in germanium. *Phys. Rev.* **87**, 387 (1952)
22. Richter, A., Glunz, S.W., Werner, F., Schmidt, J., Cuevas, A.: Improved quantitative description of Auger recombination in crystalline silicon. *Phys. Rev. B* **86**, 165202 (2012)
23. Kane, D.E., Swanson, R.M.: Measurement of the emitter saturation current by a contactless photoconductivity decay method. In: Conference Rec. 18th IEEE Photovoltaic Specialists Conf, Las Vegas, USA, pp. 578–583 (1985)

<http://www.springer.com/978-3-319-32520-0>

New Perspectives on Surface Passivation:

Understanding the Si-Al<sub>2</sub>O<sub>3</sub> Interface

Black, L.E.

2016, XXVIII, 204 p. 100 illus., 17 illus. in color.,

Hardcover

ISBN: 978-3-319-32520-0